



HAL
open science

Combining multiple data sets to unravel the spatio-temporal dynamics of a data-limited fish stock.

Cecilia Pinto, Morgane Travers-Trolet, Jed Macdonald, Etienne Rivot, Youen Vermard

► To cite this version:

Cecilia Pinto, Morgane Travers-Trolet, Jed Macdonald, Etienne Rivot, Youen Vermard. Combining multiple data sets to unravel the spatio-temporal dynamics of a data-limited fish stock.. Canadian Journal of Fisheries and Aquatic Sciences, 2019, 76 (8), pp.1338-1349. 10.1139/cjfas-2018-0149 . hal-01891429

HAL Id: hal-01891429

<https://institut-agro-rennes-angers.hal.science/hal-01891429>

Submitted on 23 May 2019

HAL is a multi-disciplinary open access archive for the deposit and dissemination of scientific research documents, whether they are published or not. The documents may come from teaching and research institutions in France or abroad, or from public or private research centers.

L'archive ouverte pluridisciplinaire **HAL**, est destinée au dépôt et à la diffusion de documents scientifiques de niveau recherche, publiés ou non, émanant des établissements d'enseignement et de recherche français ou étrangers, des laboratoires publics ou privés.

Combining multiple data sets to unravel the spatio-temporal dynamics of a data-limited fish stock.

Pinto Cecilia ^{1,2,*}, Travers-Trolet Morgane ², Macdonald Jed ³, Rivot Etienne ⁴, Vermard Youen ⁵

¹ European Commission Joint Research Centre Ispra Sector, 99013, D Sustainable Resources -D.02 Water and Marine Resources, Via Enrico Fermi 2749, Ispra, Italy

² IFREMER, 150, quai Gambetta, BP 699, F-62321 Boulogne-sur-Mer, cedex, France

³ University of Iceland, Faculty of Life and Environmental Sciences, Reykjavik, Iceland

⁴ Agrocampus Ouest, UMR 0985 INRA / Agrocampus Ouest ESE, Agrocampus, Ecologie Halieutique, 65, rue de St Briec, Rennes, France

⁵ IFREMER, Unité EMH, Rue de l'île d'Yeu, Nantes, France

* Corresponding author : Cecilia Pinto, email addresses : cecilia.pinto@ec.europa.eu ; pntccl@gmail.com

Abstract :

The biological status of many commercially-exploited fishes remains unknown, mostly due to a lack of data necessary for their assessment. Investigating the spatio-temporal dynamics of such species can lead to new insights into population processes, and foster a path towards improved spatial management decisions. Here, we focused on striped red mullet (*Mullus surmuletus*), a widespread, yet data-limited species of high commercial importance. Aiming to quantify range dynamics in this data-poor scenario, we combined fishery-dependent and -independent datasets through a series of Bayesian mixed-effects models designed to capture monthly and seasonal occurrence patterns near the species' northern range limit across 20 years. Combining multiple datasets allowed us to cover the entire distribution of the northern population of *Mullus surmuletus*, exploring dynamics at different spatio-temporal scales, and identifying key environmental drivers (i.e. sea surface temperature, salinity) that shape occurrence patterns. Our results demonstrate that even when process and/or observation uncertainty is high, or when data is sparse, by combining multiple datasets within a hierarchical modelling framework accurate and useful spatial predictions can still be made.

55 **Introduction**

56 Long-term time series are a valuable resource for testing hypotheses on how temporal
57 variability in recruitment or abundance, or patterns of range expansion or distributional shift
58 may relate to climatic and anthropogenic events (Doney et al. 2012; Hawkins et al. 2013). This
59 is a prerequisite to forecast the response of populations under future scenarios of environmental
60 change and additional anthropogenic pressures, such as fishing pressure (Szuwalski and Punt
61 2015).

62 Many fish stocks targeted by fisheries are not subjected to standardized assessment methods
63 (Costello et al. 2012), meaning that both their exploitation level and their resilience to
64 exploitation are uncertain. Non-assessed stocks not only comprise species of low commercial
65 importance; some highly exploited species also fall outside the assessment process. This
66 situation is often due to data scarcity, driven either by a lack of government investment in the
67 fisheries management process, or through the history of the data collection itself (Hilborn and
68 Ovando 2014).

69 Stock assessment methods for so-called data limited stocks (DLS) have received considerable
70 interest in recent years, with the development of new methods based on life history traits (e.g.
71 body-size frequencies), or trends in abundance and fleets (ICES 2017; Kokkalis et al. 2017).
72 However, data are still missing for many species, or have only been monitored over short time
73 scales. This critically hampers any evaluation process, and potentially reduces viability of fish
74 populations and associated fisheries (Costello et al. 2012).

75 When data collection on a species is sparse or limited, combining multiple data sources within
76 a single analysis can help to overcome the limitation of single data sets considered separately.
77 According to their respective spatio-temporal coverage, combining data sets it allows for
78 extending the time series, widening the area covered, and ultimately improving the power of

79 the analysis and our understanding of population dynamics. The development of integrated
80 analysis (as defined in Maunder and Punt (2013)) as a tool to combine different data sources
81 arising from different sampling methods (with their own spatial and temporal heterogeneity)
82 within a single framework has received attention in the statistical ecology literature (McGeoch
83 and Gaston 2002) and in fisheries sciences (Maunder and Punt 2013 and references therein).
84 Hierarchical modelling approaches explicitly separate out process models from observation
85 models, and therefore offer an efficient framework for combining multiple datasets. The process
86 equations allow for modelling multiple dependencies and stochasticity in a hierarchy of scales
87 suitable to depict the spatial and temporal variability present within the data through latent
88 parameters, whilst the set of observation equations define how the data relate to the state
89 variables of the model (Gelfand 2012; Parent and Rivot 2013; Kéry and Royle 2016). This class
90 of models is also particularly well suited to capturing residual correlation patterns through
91 inclusion of spatial (or temporal) correlation structure in the latent variables (Legendre 1993;
92 Elith and Leathwick 2009; Thorson and Minto 2015). Bayesian inferences on hierarchical
93 models offer additional technical convenience, and provide inferences in a probabilistic
94 rationale that fully propagates uncertainty (Punt and Hilborn 1997; Harwood and Stockes
95 2003).

96 In this paper, we combine four fishery-dependent and fishery-independent datasets, spanning a
97 20-year period, within a single hierarchical model to explore monthly and seasonal occurrence
98 patterns of striped red mullet (*Mullus surmuletus*, Linnaeus, 1758), a demersal Mullid of high
99 commercial importance. We focus on the “northern subpopulation” that resides in the North
100 Sea and Eastern English Channel, and shows little mixing with the “southern subpopulation”
101 (Bay of Biscay) (Mahé et al. 2014) and the “mixing zone subpopulation” (Celtic Sea and the
102 Western English Channel) (Benzinou et al. 2013). Despite being commercially targeted across
103 much of its range, information on the sensitivity of this species to changing environmental

104 conditions is scarce. The hypothesized role of dynamic gradients (e.g. sea surface temperature)
105 in shaping the migration and distribution patterns of the northern subpopulation (Beare et al.
106 2005; Engelhard et al. 2011) needs further enquiry using data covering the full geographic range
107 of the subpopulation, over several years. This northern subpopulation is also characterized by
108 strong oscillations in abundance between consecutive years (Mahé et al. 2005). During the last
109 five years, fluctuations have increased in magnitude, concurrently with the loss of the oldest
110 and most efficient spawners from the population (ICES 2015). These indices suggest an effect
111 of overexploitation (Iglésias et al. 2010) and are an alarm bell for future (and perhaps
112 prolonged) depletion. Implementation of restrictive management options are currently debated,
113 such as implementation of quota sharing within the total allowable catch (TAC) for the
114 subpopulation, as already established in a multilateral context for other species in the North Sea
115 (Hannesson 2013).

116 Indications of a depleted population state, high abundance variability and high uncertainty
117 regarding spatial distribution drivers constitute strong motivations to fill in the gaps in
118 biological and ecological knowledge for this species, and eventually provide more reliable
119 scientific advice for fisheries management. More specifically, the objectives of our study are
120 twofold: 1) to clarify the role of environmental factors on shaping occurrence patterns across
121 the full distributional range of the northern subpopulation of striped red mullet; and 2) to gain
122 insight into the mechanisms underpinning the marked inter-annual fluctuations and seasonal
123 migrations that characterize its spatio-temporal dynamics.

124 **Materials and Methods**

125 **Presence / absence data**

126 Our data are derived from three scientific bottom-trawl surveys and one set of commercial
127 fishery catch records. The scientific surveys were the winter and summer International Bottom

128 Trawl Survey (IBTS) (ICES 2012) and the Channel Ground Fish Survey (CGFS) (Coppin and
129 Travers-Trolet 1989). The IBTS surveys take place over one month across January and
130 February (winter survey, IBTS-Q1), and one month across August and September (summer
131 survey, IBTS-Q3) and cover the whole of the North Sea. Since 2007, the winter survey has been
132 expanded into the Eastern English Channel. The CGFS takes place over one month in October,
133 and has covered the Eastern English Channel since 1990. As the North Sea was not
134 systematically sampled twice a year prior to 1995, only survey data from 1995 to 2015 are
135 considered here. The commercial data come from the OBSMER French program (Cornou et al.
136 2016) which aims to collect data on landings and discards through onboard observers at sea.
137 Catch data were collected throughout the year (for every fishing operation on each sampled
138 trip) from 2003 to 2015.

139 The four initial datasets were first reclassified into two new datasets based on their spatial and
140 temporal coverage. Dataset A (n=8391) comprises observations from IBTS-Q1, IBTS-Q3,
141 CGFS and OBSMER covering the Eastern English Channel and the southern North Sea (Fig.
142 1) and spanning 1995 to 2015 at a monthly resolution. Dataset B (n=13853) has the same
143 temporal coverage (1995-2015) and covers a larger spatial area than Dataset A as it includes
144 the whole of the North Sea, but at the cost of making use of fishery-independent records only
145 (i.e. IBTS-Q1, IBTS-Q3 and CGFS) and with a seasonal (i.e. winter, summer and autumn)
146 resolution (Fig. 1). The number of records available from each data source is presented in Table
147 S1.

148 For both datasets A and B, georeferenced point records describing the catches of striped red
149 mullet captured at a particular location s , and time t , were transformed to presence/absence
150 records. This is a critical simplification to limit the effect of heterogeneity in fishing effort and
151 catchability among the various data sets, and allows us to consider that all sampling methods
152 are equivalently informative relative to the presence/absence of the species. To further limit

153 heterogeneity in the catchability and avoid “false zeros” due to low catchability (Martin et al.
154 2005) when using OBSMER data, only records from bottom-trawlers using a mesh size between
155 70-90mm were extracted for the analysis, as larger mesh sizes are typically used by boats
156 targeting other species (e.g. *Pollachius virens*).

157 **Environmental covariates**

158 Presence/absence records were correlated with a set of environmental covariates thought to
159 influence the occurrence of striped red mullet: depth at seabed, sediment type, sea surface
160 temperature (SST) and sea surface salinity (SSS). Depth at seabed was extracted from the
161 NORwegian ECOlogical Model system (NORWECOM) database
162 (<http://www.imr.no/~morten/wgoofe/>). SSS was extracted at a monthly resolution from the
163 NORWECOM website for the time interval from 1990 to 2008, while data for 2009-2015 were
164 obtained by contacting the author of the model system directly. The SST data were obtained
165 from satellite observations at a daily resolution, but for the purposes of this study a monthly
166 mean was computed. Data for 1990-2008 was extracted from the AVHRR Pathfinder Version
167 5.2 (PFV5.2) dataset, provided by the US National Oceanographic Data Center and GHRSSST
168 (<http://pathfinder.nodc.noaa.gov>) (Casey et al. 2010), while the 2009-2015 SST data was
169 extracted from the ODYSSEA processing chain operated within the ESA/MEDSPIRATION
170 project (Gohin et al. 2010). Seabed sediment types were adapted from Larssonneur et al. (1982)
171 and Schluter and Jerosch (2008), and reclassified into five broad categories: mud, fine sand,
172 coarse sand, gravel and pebbles. To test for collinearity among covariates, we used the ‘vif.mer’
173 function (VIF threshold set to 10) on a model object fitted using the ‘lme4’ package (Bates et
174 al. 2015) in R version 3.3.0 (R Core Team 2016), to calculate variance inflation factors for each
175 predictor (R code available here: <https://github.com/aufrank/R-hacks/blob/master/mer-utils.R>
176). As no collinearity among variables was detected, variance inflation factor values are not
177 shown in the results.

178 **Modelling striped red mullet occurrence**

179 Dataset A and Dataset B were analysed independently but using the same modelling approach.

180 Models were built in a hierarchical Bayesian framework using the SPDE (Stochastic Partial

181 differential Equations) approach in the ‘R-INLA’ package (<http://www.r-inla.org>) (Rue et al.

182 2009; Lindgren et al. 2011; Lindgren and Rue 2015) in R. This approach provides direct

183 inference on the spatial and temporal dependencies in the data. The process equation models

184 the probability, $p_t(s)$, of striped red mullet presence at time-step t (i.e. either month or season)

185 and location s , as a random field on the logit scale:

186 (1)
$$\text{logit}(p_t(s)) = X_t(s) \times \beta + \theta_t(s)$$

187 where $X_t(s)$ represents a vector of covariates (depth at seabed, sediment, SST, SSS) at time-step

188 t and at location s , β represents a vector of coefficients (fixed effects) to be estimated, and $\theta_t(s)$

189 is a spatio-temporal random effect to account for variation not explicitly explained by

190 covariates. Random effects are defined by a Gaussian random field that is spatially

191 autoregressive (depending on the distance between locations) and temporally uncorrelated (for

192 details see Cameletti et al., 2013). To avoid computational costs that rapidly arise in continuous

193 space (the so called big-n problem (Lasinio et al. 2013)), the spatial covariation is modelled

194 within a Gaussian Markov random field (GMRF) on a discrete mesh, that defines the area of

195 interest (Krainski et al. 2016) (see Fig. S2). This way the influence of spatial covariance at any

196 point s is reduced to a set of neighbours (Cameletti et al. 2013).

197 Given the latent field of presence probability $p_t(s)$ at any time t and location s , presence/absence

198 data $y_t(s)$ are modelled as mutually independent and identically distributed Bernoulli variables

199 (2)
$$y_t(s) \sim \text{Bernoulli}(p_t(s))$$

200 The full likelihood equation for the model then arises from the product of Bernoulli for all raw
201 data (eq. 2). Because all data sources are considered as presence/absence, the strength of the
202 hierarchical structure is that different data sources are integrated within a single analysis to infer
203 a unique random field model for the probability of presence that captures the spatio-temporal
204 covariations as defined in eq. (1).

205 Within the SPDE approach, eq. 1 can be rewritten as:

$$206 \quad (3) \quad \text{logit}(p_t(s)) = X_t(s)\beta + A_t(s)\theta_t$$

207 where observation matrix $A_t(s)$ is directly related to the space discretizing mesh (Fig. S2) as it
208 extracts the values of the spatio-temporal random field at each location s and at each time-step
209 t . The realization of the random field can be represented through its mean density distribution
210 and standard deviation which in turn can be translated as the level of uncertainty at a certain
211 location depending on the availability of data points (Cameletti et al. 2013). The quantification
212 of such uncertainty, through the realization of the random field, allowed us to account for the
213 heterogeneity across time and space of the sampling design, originating from the integration of
214 different datasets.

215 Different mesh designs were compared visually and the sensitivity of parameter estimation to
216 the different designs assessed (Cosandey-Godin et al. 2015). The best mesh designs for each
217 dataset (see Fig. S1) includes an outer extension to avoid a “boundary effect” (Lindgren and
218 Rue 2015) and regularly-shaped triangles, both in the inner and in the outer extension, and at
219 the border between the two extensions (Krainski et al. 2016). Once the best mesh was selected,
220 parameters values defining it were kept constant across models (i.e. at the same spatial
221 resolution).

222 The simplified Laplace method was used to approximate the posterior marginal distributions
223 (for details see Martins et al. 2013). We built and compared models of increasing complexity,
224 from the null model including no covariates to the full model including all covariates and
225 random effects. Models were compared through deviance information criterion (DIC), the log
226 marginal likelihood and by estimating the variance contribution of random effects against that
227 of fixed effects. To evaluate out-of-sample predictive capacity for each fitted model, we derived
228 the conditional predictive ordinate (CPO), defined as the cross-validated (cv) predictive density
229 at observation $y_t(s)$ with that observation removed (Roos and Held 2011). We used the CPO
230 values to compute the cv logarithmic score (Gneiting and Raftery 2007), a measure of predictive
231 quality, and the cv Brier score (i.e. mean prediction error) for each model. This latter score
232 evaluates the correspondence between fitted probabilities and observed binary outcomes
233 (Schmid and Griffith 2005, Roos and Held 2011). Lower values on both scores reflect better
234 predictions, with the Brier score interpreted relative to a reference value equal to sampling
235 prevalence. The probability of presence was predicted across the whole area covered by each
236 dataset, but here we limit our spatial predictions to the areas where the standard deviation of
237 the response was smaller than its mean value, also corresponding to the end of the asymptotic
238 phase of its distribution (Fig. S3). Following Ward et al. (2015), we also estimated the
239 predictive accuracy of the best model through the area under the receiver operating
240 characteristic curve (AUC) using the ‘ROCR’ package (Sing et al. 2005).

241 **Priors**

242 We used the default priors for the fixed effects and hyperparameters as implemented in R-INLA
243 (described in Lindgren and Rue 2015). Hyperparameters currently constitute an active area of
244 research for the R-INLA team (see R-INLA documentation available at <http://www.r-inla.org/>).
245 The latent field parameters θ_1 and θ_2 were defined by a multivariate normal distribution which

246 is a combination of $\theta_1=N(0,10)$, $\theta_2=N(0,10)$. All fixed parameter priors were defined by a
247 $N(0,1000)$ except the intercept that has a prior distribution $N(0,\infty)$.

248 **Results**

249 **Model selection**

250 Models with a month within year structure (for dataset A) and season within year (for dataset
251 B) structure for the random effect were always preferred based on DIC. Models including all
252 environmental covariates were selected as the best models on the balance of the DIC, the log
253 marginal likelihood estimates, the reduced variance contribution of the spatial effect and
254 predictive quality (CVLS and Brier score) (Table 1). The spatial correlation range (nominal
255 range) of the best model for dataset A was 2.66 decimal degrees, and 8.51 for dataset B (Table
256 1). The AUC estimated for the best model for dataset A was 0.61, and 0.69 for dataset B.

257 **Environmental parameters**

258 SST and SSS were both found to be positively correlated with the presence of striped red mullet
259 for dataset A while for dataset B only SST was significant (Table 2), suggesting that this species
260 has a preference for areas where waters are warmer and more saline. Sediment types were not
261 correlated with the presence of striped red mullet at the monthly time scale for dataset A or at
262 a seasonal scale for dataset B (Table 2). Finally, depth at seabed had no effect on the distribution
263 of striped red mullet at both resolutions.

264 **Spatial latent field**

265 Posterior estimates of the spatial random effects inform about the spatio-temporal variability
266 that is not captured by the effects of covariates in the model. Results are presented from 2009
267 onwards to allow direct comparison between datasets, as data for all months and seasons are
268 available since 2009 only.

269 For dataset A, posterior estimates of the spatial random effect revealed that the northern
270 subpopulation of striped red mullet changed its distribution month by month, moving into and
271 out of the Eastern English Channel (Fig. 2). Due to the high variation of the monthly
272 distributional pattern among years, it is difficult to identify a consistent monthly movement
273 trend across areas. For dataset B in which sampling is consistent between winter and summer,
274 results revealed a seasonal migration of the population moving from the north-east in the winter
275 to the south in the summer, but with higher uncertainty during autumn, as data are available
276 only for the Eastern English Channel (Fig. 3). Random effects are estimated with higher
277 uncertainty for dataset A than for data set B (Fig. 3, 4), as a consequence of the higher spatial
278 variability inherent in commercial sampling and fewer observations per month, as compared
279 with the more spatially-consistent survey observations in dataset B.

280 **Predicted probability of presence**

281 Our modelling framework also allows for predicting the probability of presence at any point in
282 the area provided that covariates are available. Figure 5 reports the predicted probability of
283 presence of striped red mullet in the area covered by dataset A, only in areas where the results
284 are more reliable. These reliable areas were defined as the ones displaying a low standard
285 deviation, i.e. low uncertainty, using a cutoff of 13.23 (the mean of the standard deviation also
286 corresponding to the upper limit of the distribution where the standard deviation is more or less
287 constant) (see also Fig. S3). Beyond the inter-annual and seasonal variability in the probability
288 of striped red mullet presence, recurrent patterns can be detected. Results highlight a strong
289 seasonal difference, with high predicted probability of presence (>70%) from July to October
290 when the surface waters are warmer and lower probability of presence (<50%) predicted for
291 colder months (late winter) (Fig. 5 and Fig. S4A). We also detected changes across years linked
292 to SST; during the coldest springs of the series (2010 and 2013) (Fig. S4B), the probability of
293 presence was lower for these seasons (Fig. 5 and Fig. S4A). Predictions also suggest large scale

294 seasonal movements of the striped red mullet across the study area. The striped red mullet seems
295 to spend the winter in the English Channel, before leaving this area in March and reaching the
296 Dover Strait by April, although this pattern varies across years. We note also that in 2015, the
297 probability of presence remains high in the English Channel throughout the year but on average,
298 there are no strong variations in the registered SSTs compared to the previous years (Fig. S4A).
299 Predictions obtained from dataset B (Fig. 6) seem contradictory as they show a much higher
300 probability of presence of striped red mullet during the winter, specifically in the north west of
301 the North Sea and the Eastern English Channel. Whilst in the summer and the autumn, the
302 probability of presence increased only in the Eastern English Channel, and, across all grid cells,
303 was 20% lower than the winter period.

304 **Discussion**

305 This study provides the first spatially-explicit analysis of how environmental parameters may
306 shape the distribution of striped red mullet near its northern range boundary. All available
307 information on this data-limited species was integrated into a single analysis that directly
308 accounts for correlation structures in the data, and the sources of uncertainty in data and process.
309 The results provide a substantive contribution to our understanding of the spatio-temporal
310 dynamics of this data-limited stock.

311 Our findings suggest that the occurrence of the northern subpopulation is positively correlated
312 with water salinity and temperature. Results for the latter covariate match suggestions by Beare
313 et al. (2005), who hypothesized that the presence of striped red mullet in northern waters in
314 winter was related to increasing surface water temperatures. Moreover, our predictions show
315 that certain years are characterized by larger occupied areas (e.g. 2011 and 2015) interspersed
316 with years of very low and/or scattered concentrations (e.g. 2013) (see Fig. 5 and 6). This
317 complements previous descriptions of the strong interannual fluctuations in abundance within

318 this subpopulation (Mahé et al. 2005, Carpentier et al. 2009). Whether range expansion is linked
319 to population size in this species (see Fisher and Frank 2004) remains an open question. Yet,
320 despite marked inter-annual variability in the distributional range, we detected patterns of
321 seasonal migrations starting in both the north-east of the North Sea and the English Channel in
322 winter, moving to the south of the North Sea in spring/summer and entering the Eastern English
323 Channel in autumn. Previous work has often focused on the effect of water temperature (and
324 other environmental parameters) on population abundances. For instance, striped red mullet has
325 increased in abundance by 30% over the last two decades in the English Channel, concomitantly
326 with a shift towards a warmer phase of the Atlantic Multidecadal Oscillation index (Auber et
327 al. 2015). Cheung et al. (2013) predicted that species preferring warmer waters will increase in
328 abundance and dominate fisheries catches in northern latitudes, as appears to be occurring in
329 species such as Atlantic mackerel (*Scomber scombrus*) and hake (*Merluccius merluccius*)
330 (Jansen 2014; Baudron and Fernandes 2015; Hughes et al. 2015).

331 However abundances are not necessarily correlated to distribution extensions. Therefore, when
332 developing spatial management frameworks to improve fisheries management, coupling the
333 dynamics of both abundance and spatial distribution will likely prove productive to move
334 forward. That said, presence-absence data are often more easily obtained and more widely
335 available than abundance data, and modelling presence-absence can make the integration of
336 data obtained from heterogeneous surveys simpler. Indeed, provided that detectability of the
337 survey method(s) is considered to be 100%, meaning that at least one individual will be captured
338 if the species is in fact present, presence-absence models allow us to largely ignore variation in
339 catchability among different survey methods and sampling gears.

340 Although results from both datasets identify a positive effect of SST on the presence of striped
341 red mullet, when looking at predictions we find that the highest probability of presence (both
342 in terms of area and absolute values) is predicted in the summer months for dataset A but not

343 for dataset B. Such discrepancy between the models built from the two datasets may result from
344 several (non-mutually exclusive) hypotheses: 1) The effect of temperature on the population
345 could be stronger in the winter than in the summer, causing the SST coefficients to vary
346 throughout the seasons; 2) Gradients in environmental factors could be steeper in dataset B than
347 in dataset A, as a direct function of the larger area covered by dataset B. This would be
348 consistent with the fact that the relative variation in DIC when including covariates in the model
349 is sharper in dataset B than in dataset A, suggesting that these have a stronger explanatory power
350 than in dataset A. This is confirmed also by the consistent contribution of the spatial variance
351 and by the increased autocorrelation range, which are not affected by the addition of covariates
352 in dataset A. 3) Last, the difference observed in model predictions between datasets could also
353 result from an effect of sampling bias. Dataset B is derived mainly from IBTS data that are
354 consistently sampled every winter and every summer. Dataset A also contains data from the
355 IBTS surveys, but is complemented by the OBSMER data. Though incorporating true absences,
356 this commercial dataset is still potentially biased by variation in nominal and spatial commercial
357 fishing effort that shifts not only between months but also between years (Fig. S6). Although
358 we cannot completely rule out seasonally-variable fishing effort as contributing to our spatial
359 predictions for dataset A, we suggest that any effects are relatively minor given our use of
360 presence-absence data as previously discussed. Building two different models based on the two
361 different datasets allows us to glean the maximum possible information from both, and improve
362 our understanding of the species' dynamics at different spatial and temporal scales. Dataset A
363 provides insight into the spatio-temporal dynamics of the northern population of striped red
364 mullet at a monthly level that could be missed using only dataset B, which instead exposes the
365 seasonal dynamics at a larger spatial scale, using spatially-consistent survey information.
366 Importantly, the lower level of sampling heterogeneity in dataset B suggests where, spatially,

367 the predictions from dataset A may be less reliable due to the high uncertainty given by non-
368 consistent sampling.

369 Integrating multiple surveys in a single dataset (either within A or B) allowed us to increase
370 both the number of observations and our capacity to detect statistical flukes (Maunder and Punt
371 2013). Moreover, comparing the results from the separate analyses of datasets A and B allowed
372 us to expand the geographical area (Eastern English Channel and Southern North Sea for dataset
373 A, whole North Sea for dataset B) and explore the consistency of our inferences across two
374 different spatial scales and at two different temporal resolutions (monthly for A, and seasonal
375 for B). As noted by Maunder and Punt (2013), when integrating multiple data sources, a trade
376 off should be found to maximize the scientific reward of integrated modelling. Integrating
377 various sources of data in the same analysis does not necessarily give rise to improved
378 understanding of the target system, as it may lead to conflicts in what the datasets tell us, in
379 addition to increasing statistical complexity and computational costs. Separating the dataset
380 built by integrating the IBTS-Q1, IBTS-Q3, CGFS and OBSMER data into two subsets which
381 differed in spatial and temporal resolution was our trade-off. Analysing dataset A alone allowed
382 us to obtain inferences at a monthly level instead of just at a seasonal level. Additionally, a
383 separate analysis of dataset A and B provided insights on the effects of environmental
384 parameters at different spatial scales.

385 The major source of uncertainty in the data came from the lack of commercial data for single
386 months in years prior to 2003 (the time series is complete for each month only from 2009
387 onwards). Confidence surrounding the estimates on this subpopulation during this time period
388 is therefore relatively low, and further efforts are needed to improve data quality. A substantial
389 impediment to progress on this front relates to the difficulties in accessing commercial catch
390 data coming from observer programs that operate in countries bordering the North Sea. The
391 advantages of having observer data from foreign fisheries targeting local stocks was

392 demonstrated in the Alaskan fisheries (French et al. 1982) and stands in stark contrast to the
393 situation in the Eastern English Channel and North Sea area, where multiple countries similarly
394 share the quota on several harvested stocks. Hannesson et al. (2013) showed that cooperation
395 always brings in more advantages than competition when stock harvesting is shared among
396 parties. Hence, strong incentive exists to integrate all the available data – both fishery dependent
397 and independent (e.g. national on board observer programs) – to maximize coverage of spatio-
398 temporal information in commercial stocks.

399 Species which are commercially exploited though not formally managed, are particularly
400 vulnerable to overexploitation as their population dynamics' are often not monitored, with no
401 limits set on landings or minimum sizes. Using striped red mullet for illustration, our results
402 have demonstrated some advantages of data integration and explicitly accounting for
403 uncertainty under data limitation; however, it is important to note that these steps alone are not
404 the silver bullet for successful fisheries management. Instead, we hope this work inspires future
405 sampling designs, data collection and multilateral data-sharing programs that in conjunction
406 with appropriate modelling approaches can lead to better adaptive management decisions for
407 data-limited populations (Walters 2007; Maunder and Punt 2013).

408 **Acknowledgements**

409 CP's postdoc was funded by Ifremer and France Filière Pêche. The authors would like to thank
410 Bruno Ernande for the suggestions and comments that improved the work during the analysis.
411 The authors also thank two anonymous reviewers for their comments which helped to improve
412 the manuscript.

413 **References**

414 Auber, A., Travers-Trolet, M., Villanueva, M.C., and Ernande, B. 2015. Regime Shift in an
415 Exploited Fish Community Related to Natural Climate Oscillations. PLoS One **10**(7):

416 e0129883. doi:10.1371/journal.pone.0129883.

417 Baudron, A.R., and Fernandes, P.G. 2015. Adverse consequences of stock recovery: European
418 hake, a new “choke” species under a discard ban? *Fish Fish.* **16**(4): 563–575.

419 doi:10.1111/faf.12079.

420 Benzinou, A., Carbini, S., Nasreddine, K., Elleboode, R., and Mahé, K. 2013. Discriminating
421 stocks of striped red mullet (*Mullus surmuletus*) in the Northwest European seas using
422 three automatic shape classification methods. *Fish. Res.* **143**: 153–160. Elsevier B.V.

423 doi:10.1016/j.fishres.2013.01.015.

424 Cameletti, M., Lindgren, F., Simpson, D., and Rue, H. 2013. Spatio-temporal modeling of
425 particulate matter concentration through the SPDE approach. *AStA Adv. Stat. Anal.* **97**:
426 109–131.

427 Casey, K.S., Brandon, T.B., Cornillon, P., and Evans, R. 2010. The Past, Present, and Future
428 of the AVHRR Pathfinder SST Program. *In Oceanography from Space, revisited*, V.
429 Barale,. pp. 323–341.

430 Cheung, W.W.L., Watson, R., and Pauly, D. 2013. Signature of ocean warming in global
431 fisheries catch. *Nature* **497**(7449): 365–368. Nature Publishing Group.

432 doi:10.1038/nature12156.

433 Coppin, F., and Travers-Trolet, M. 1989. CGFS : CHANNEL GROUND FISH SURVEY.

434 Available from <http://dx.doi.org/10.18142/11>.

435 Cornou, A.-S., Diméet, J., Goascoz, N., Quinio-Scavinner, M., and Rochet, M.-J. 2016.

436 Captures et rejets des métiers de pêche français Resultats des observations a bord des
437 navires de pêche professionnelle en 2015. *In OBSMER*.

- 438 Cosandey-Godin, A., Krainski, E.T., Worm, B., and Flemming, J.M. 2015. Applying
439 Bayesian spatiotemporal models to fisheries bycatch in the Canadian Arctic. *Can. J. Fish.*
440 *Aquat. Sci.* **72**(2): 186–197. doi:10.1139/cjfas-2014-0159.
- 441 Costello, C., Ovando, D., Hilborn, R., Gaines, S.D., Deschenes, O., and Lester, S.E. 2012.
442 Status and solutions for the world's unassessed fisheries. *Science* (80-.). **338**: 517–520.
443 doi:10.1126/science.1223389.
- 444 Doney, S.C., Ruckelshaus, M., Emmett Duffy, J., Barry, J.P., Chan, F., English, C.A.,
445 Galindo, H.M., Grebmeier, J.M., Hollowed, A.B., Knowlton, N., Polovina, J., Rabalais,
446 N.N., Sydeman, W.J., and Talley, L.D. 2012. Climate Change Impacts on Marine
447 Ecosystems. *Ann. Rev. Mar. Sci.* **4**(1): 11–37. doi:10.1146/annurev-marine-041911-
448 111611.
- 449 Elith, J., and Leathwick, J.R. 2009. Species Distribution Models: Ecological Explanation and
450 Prediction Across Space and Time. *Annu. Rev. Ecol. Evol. Syst.* **40**(1): 677–697.
451 doi:10.1146/annurev.ecolsys.110308.120159.
- 452 French, R., Nelson Jr., R., and Wall, J. 1982. Role of the United States Observer Program in
453 management of foreign fisheries in the Northeast Pacific Ocean and Eastern Bering Sea.
454 *North Am. J. Fish. Manag.* **2**(August): 122–131. doi:10.1577/1548-
455 8659(1982)2[122:ROTUSO]2.0.CO;2.
- 456 Gelfand, A.E. 2012. Hierarchical modeling for spatial data problems. *Spat. Stat.* **1**: 30–39.
457 Elsevier Ltd. doi:10.1016/j.spasta.2012.02.005.
- 458 Gneiting, T., and Raftery, A.E. 2007. Strictly proper scoring rules, prediction, and estimation.
459 *J. Am. Stat. Assoc.* **102**: 359–378.
- 460 Gohin, F., Saulquin, B., and Bryere, P. 2010. Atlas de la Température, de la concentration en

- 461 Chlorophylle et de la Turbidité de surface du plateau continental français et de ses abords
462 de l'Ouest européen. : 53.
- 463 Hannesson, R. 2013. Sharing a migrating fish stock. *Mar. Resour. Econ.* **28**(1): 1–17.
- 464 Hawkins, S.J., Firth, L.B., McHugh, M., Poloczanska, E.S., Herbert, R.J.H., Burrows, M.T.,
465 Kendall, M.A., Moore, P.J., Thompson, R.C., Jenkins, S.R., Sims, D.W., Genner, M.J.,
466 and Mieszkowska, N. 2013. Data rescue and re-use: Recycling old information to
467 address new policy concerns. *Mar. Policy* **42**: 91–98. doi:10.1016/j.marpol.2013.02.001.
- 468 Heessen, H.J.L., Dalskov, J., and Cook, R.M. 1997. The International Bottom Trawl Survey
469 in the North Sea, the Skagerrak and Kattegat. *ICES C. Y*: 31.
- 470 Hilborn, R., and Ovando, D. 2014. Reflections on the success of traditional fisheries
471 management. *ICES J. Mar. Sci.* **71**(5): 1040–1046. doi:10.1093/icesjms/fsu034.
- 472 Hughes, K.M., Dransfeld, L., and Johnson, M.P. 2015. Climate and stock influences on the
473 spread and locations of catches in the northeast Atlantic mackerel fishery. *Fish.*
474 *Oceanogr.* **24**(6): 540–552. doi:10.1111/fog.12128.
- 475 ICES. 2017. Report of the ICES Workshop on the Development of Quantitative Assessment
476 Methodologies based on Life-history traits, exploitation characteristics, and other
477 relevant parameters for stocks in categories 3–6 (WKLIFEVI). 3–7 October 2016,
478 Lisbon, Portugal.
- 479 Iglésias, S.P., Toulhoat, L., and Sellos, D.Y. 2010. Taxonomic confusion and market
480 mislabelling of threatened skates: important consequences for their conservation status.
481 *Aquat. Conserv. Mar. Freshw. Ecosyst.* **20**(3): 319–333. doi:10.1002/aqc.1083.
- 482 Jansen, T. 2014. Pseudocollapse and rebuilding of North Sea mackerel (*Scomber scombrus*).

483 ICES J. Mar. Sci. **71**(2): 299–307. doi:10.1093/icesjms/fst034.

484 Kéry, M., and Royle, J.A. 2016. Chapter 2 - What Are Hierarchical Models and How Do We
485 Analyze Them? *In Applied Hierarchical Modeling in Ecology*.

486 doi:http://dx.doi.org/10.1016/B978-0-12-801378-6.00002-3.

487 Krainski, E.T., Lindgren, F., Simpson, D., and Rue, H. 2016. The R-INLA tutorial : SPDE
488 models. doi:10.1093/biomet/asv064.

489 Larssonneur, C., Bouysse, P., and Auffret, J.P. 1982. The superficial sediments of the English
490 Channel and its Western Approaches. *Sedimentology* **29**: 851–864.

491 Legendre, P. 1993. Spatial Autocorrelation : Trouble or New Paradigm ? *Ecology* **74**(6):
492 1659–1673.

493 Lindgren, F., and Rue, H. avar. 2015. Bayesian Spatial Modelling with R-INLA. *J. Stat.*
494 *Softw.* **63**(19): 1–26. doi:10.18637/jss.v063.i19.

495 Mahé, K., Destombes, A., Coppin, F., Koubbi, P., Vaz, S., Roy, D.L., and Carpentier, A.
496 2005. Le rouget barbet de roche *Mullus surmuletus* (L. 1758) en Manche orientale et mer
497 du Nord. *Ifremer/Crpmem* **39**: 1–199.

498 Mahe, K., Villanueva, M.C., Vaz, S., Coppin, F., Koubbi, P., and Carpentier, A. 2014.
499 Morphological variability of the shape of striped red mullet *Mullus surmuletus* in
500 relation to stock discrimination between the Bay of Biscay and the eastern English
501 Channel. *J. Fish Biol.* **84**(4): 1063–1073. doi:10.1111/jfb.12345.

502 Martins, T.G., Simpson, D., Lindgren, F., and Rue, H. 2013. Bayesian computing with INLA:
503 New features. *Comput. Stat. Data Anal.* **67**: 68–83. Elsevier B.V.

504 doi:10.1016/j.csda.2013.04.014.

- 505 Maunder, M.N., and Punt, A.E. 2013. A review of integrated analysis in fisheries stock
506 assessment. *Fish. Res.* **142**: 61–74. Elsevier B.V. doi:10.1016/j.fishres.2012.07.025.
- 507 McGeoch, M.A., and Gaston, K.J. 2002. Occupancy frequency distributions: patterns,
508 artefacts and mechanisms. *Biol. Rev.* **77**(3): 311–331. doi:10.1017/s1464793101005887.
- 509 R Core Team. 2016. R: A language and environment for statistical computing. R Foundation
510 for Statistical Computing. Vienna, Austria. Available from <https://www.r-project.org/>.
- 511 Roos, M., and Held, L. 2011. Sensitivity analysis in Bayesian generalized linear mixed
512 models for binary data. *Bayesian Anal.* **6**: 259–278.
- 513 Schluter, M., and Jerosch, K. 2008. Digital atlas of the North Sea (DANS). Geo-information
514 regarding geology, geochemistry, oceanography and biology. Available from
515 http://www.awi.de/en/research/research_divisions/geosciences/marine_geochemistry/marine_gis/digital_atlas_of_the_north_sea/.
- 517 Schmid, C.H., and Griffith, J.L. 2005. Multivariate classification rules: calibration and
518 discrimination. *In* Encyclopedia of Biostatistics, second edition. *Edited by* P. Armitage
519 and T. Colton. John Wiley & Sons, London, UK pp. 3491–3497.
- 520 Sing, T., Sander, O., Beerenwinkel, N., and Lengauer, T. 2005. ROCr: visualizing classifier
521 performance in R. *Bioinformatics* **21**(20): 7881 pp. Available from [http://rocr.bioinf.mpi-](http://rocr.bioinf.mpi-sb.mpg.de)
522 [sb.mpg.de](http://rocr.bioinf.mpi-sb.mpg.de).
- 523 Szuwalski, C.S., and Punt, A.E. 2015. Can an aggregate assessment reflect the dynamics of a
524 spatially structured stock? Snow crab in the eastern Bering Sea as a case study. *Fish.*
525 *Res.* **164**: 135–142. Elsevier B.V. doi:10.1016/j.fishres.2014.10.020.
- 526 Thorson, J.T., and Minto, C. 2015. Mixed effects: a unifying framework for statistical

527 modelling in fisheries biology. ICES J. Mar. Sci. **72**(5): 1245–1256.

528 doi:10.1093/icesjms/fst176.

529 Walters, C.J. 2007. Is Adaptive Management Helping to Solve Fisheries Problems? *AMBIO*

530 *A J. Hum. Environ.* **36**(4): 304–307. doi:10.1579/0044-

531 7447(2007)36[304:iamhts]2.0.co;2.

532

533

Draft

535 Table 1 Models' DIC and log marginal likelihood, estimated spatial autocorrelation range (ρ
 536), variance contribution of the spatial effect to the total variance (σ^2), cross-validated
 537 logarithmic score (CVLS) and Brier score. Best models for each dataset are highlighted in grey.

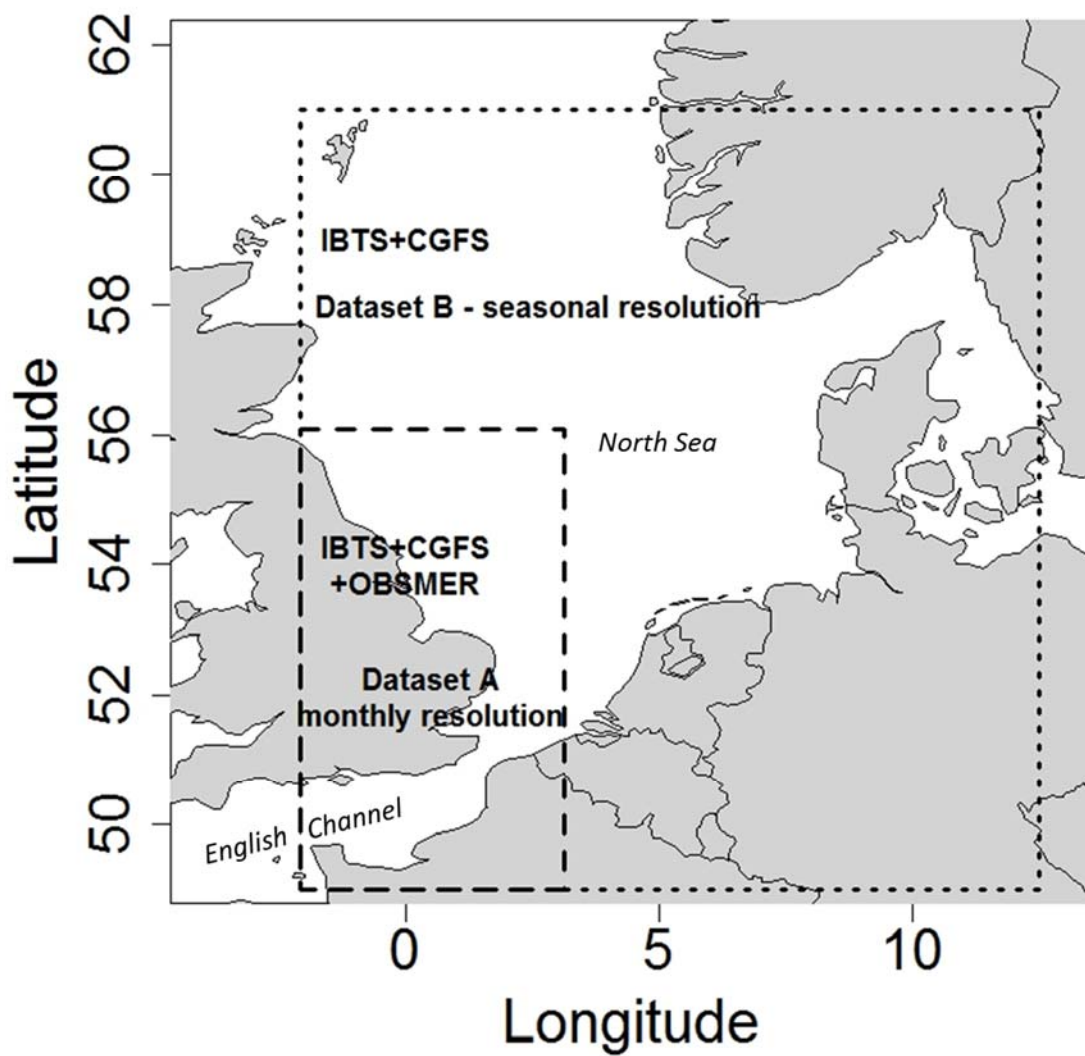
DATASET A	DIC	LOG MARGINAL LIK	ρ SPATIAL EFFECT	σ^2 SPATIAL EFFECT	CVLS	BRIER SCORE
SED+DEP+SSS+SST	7529	-4204	2.656599	4.604428	0.4468516	0.07572407
SED+DEP+SSS	7556	-4222	2.768245	4.856019	0.4482658	0.1461075
SED+DEP	7558	-4219	2.726399	4.836133	0.4483667	0.1460957
SED	7557	-4210	2.770354	4.879648	0.4483378	0.1460749
SSS+SST	7541	-4221	2.431589	5.182673	0.4471932	0.1457849
NO COVS	7569	-4237	2.553919	5.495750	0.4486286	0.146228
DATASET B	DIC	LOG MARGINAL LIK	ρ SPATIAL EFFECT	σ^2 SPATIAL EFFECT	CVLS	BRIER SCORE
SED+DEP+SSS+SST	6881	-3841	8.509531	6.554891	0.2532677	0.07857798
SED+DEP+SSS	6894	-3854	8.01782	6.658798	0.2536428	0.07861613
SED+DEP	6895	-3848	8.000895	6.626146	0.2536606	0.07861056
SED	6900	-3839	7.889699	6.483401	0.2538337	0.0786736
SSS+SST	7672	-4257	7.474648	6.46565	0.2467375	0.05887704
NO COVS	7021	-3907	7.213805	6.803004	0.2583787	0.08070601

538 Table 2 Estimated coefficients for the best models of dataset A and dataset B. Values are
 539 posterior means and intervals (CI) are 95% Bayesian Credibility Intervals. Intervals not
 540 containing 0 are highlighted in bold.

	Dataset A	Dataset B
	Mean (95% CI)	Mean (95% CI)
Mud	-4.4276 (-30.0362 ; +21.0294)	-0.7849 (-26.1550; +24.4351)
Fine sand	-4.5374 (-30.1481;+ 20.9218)	-0.8095 (-26.1797; +24.4106)
Gravels	-4.0908 (-29.7055;+ 21.3721)	-0.6337 (-26.0048; +24.5872)
Pebbles	-5.0858 (-30.6998; +20.3766)	-1.7490 (-27.1200; +23.4718)
Coarse sand	-3.8629 (-29.4751; +21.5977)	0.3191 (-25.0513; +25.5395)
SST	0.2079 (0.1506; 0.2656)	0.2680 (0.1805 ; 0.3560)
SSS	0.6516 (0.0340; 1.2665)	-0.0629 (-0.1820; +0.0558)
Depth	-0.0054 (-0.0136; +0.0027)	0.0022 (-0.0015; +0.0058)

541

543 Figure 1 Spatial coverage of the two datasets, A and B.



544

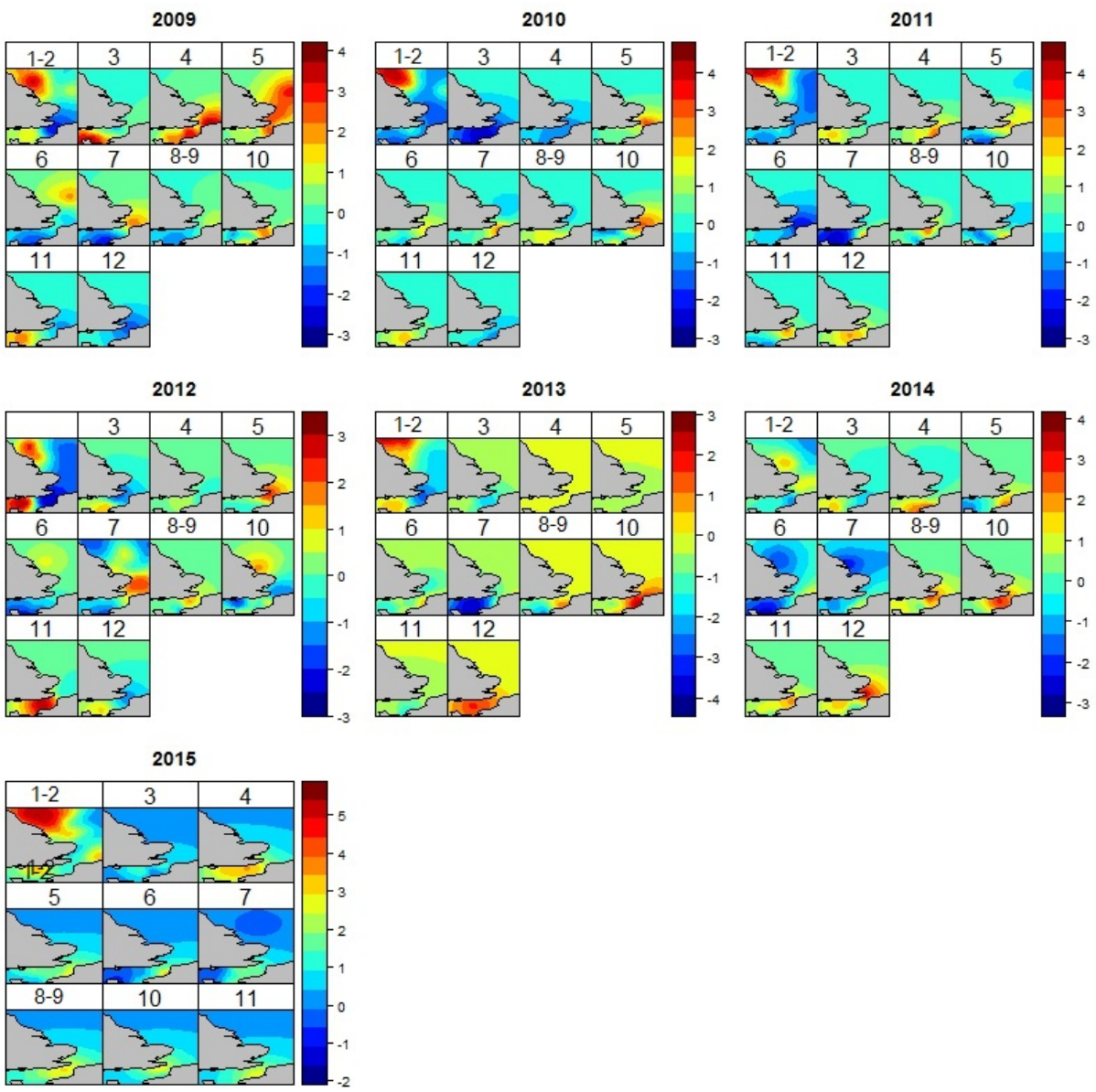
545

546

547

548 Figure 2 Posterior mean of the spatial random effect for dataset A – positive values indicate a
549 high density of presence data while negative values indicate a high density of absence data.
550 The months of January, February and August, September were grouped together in order to
551 combine the parts of the IBTS survey that straddled months.

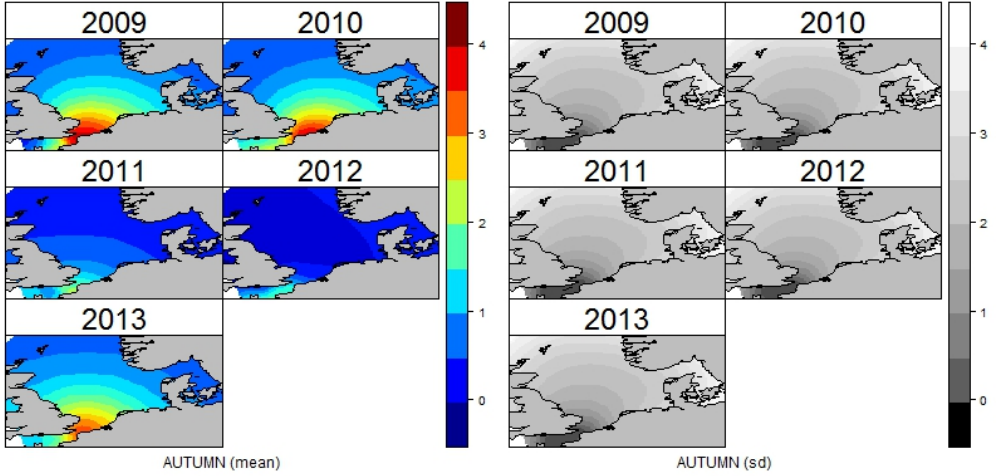
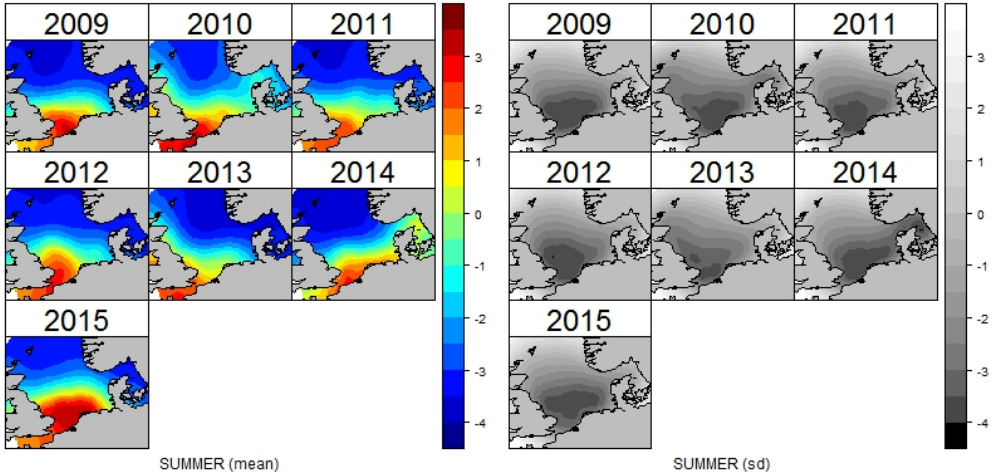
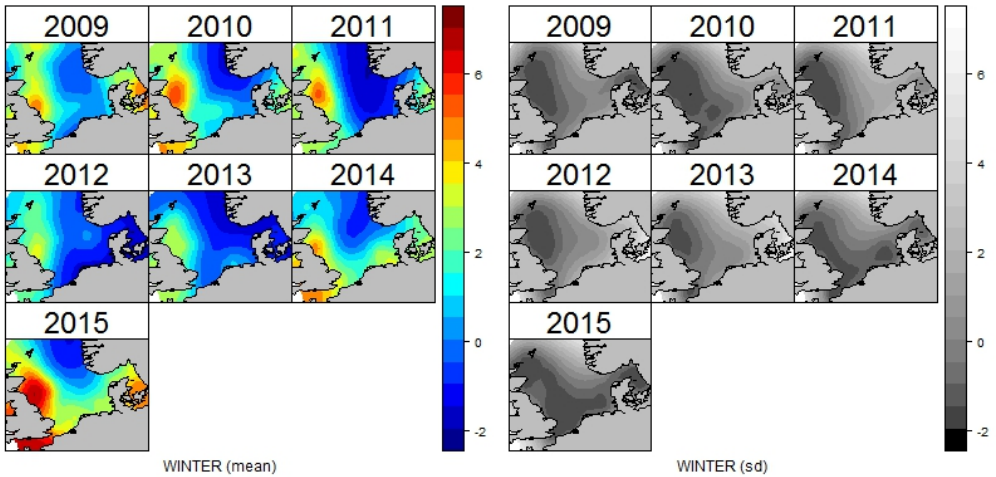
552



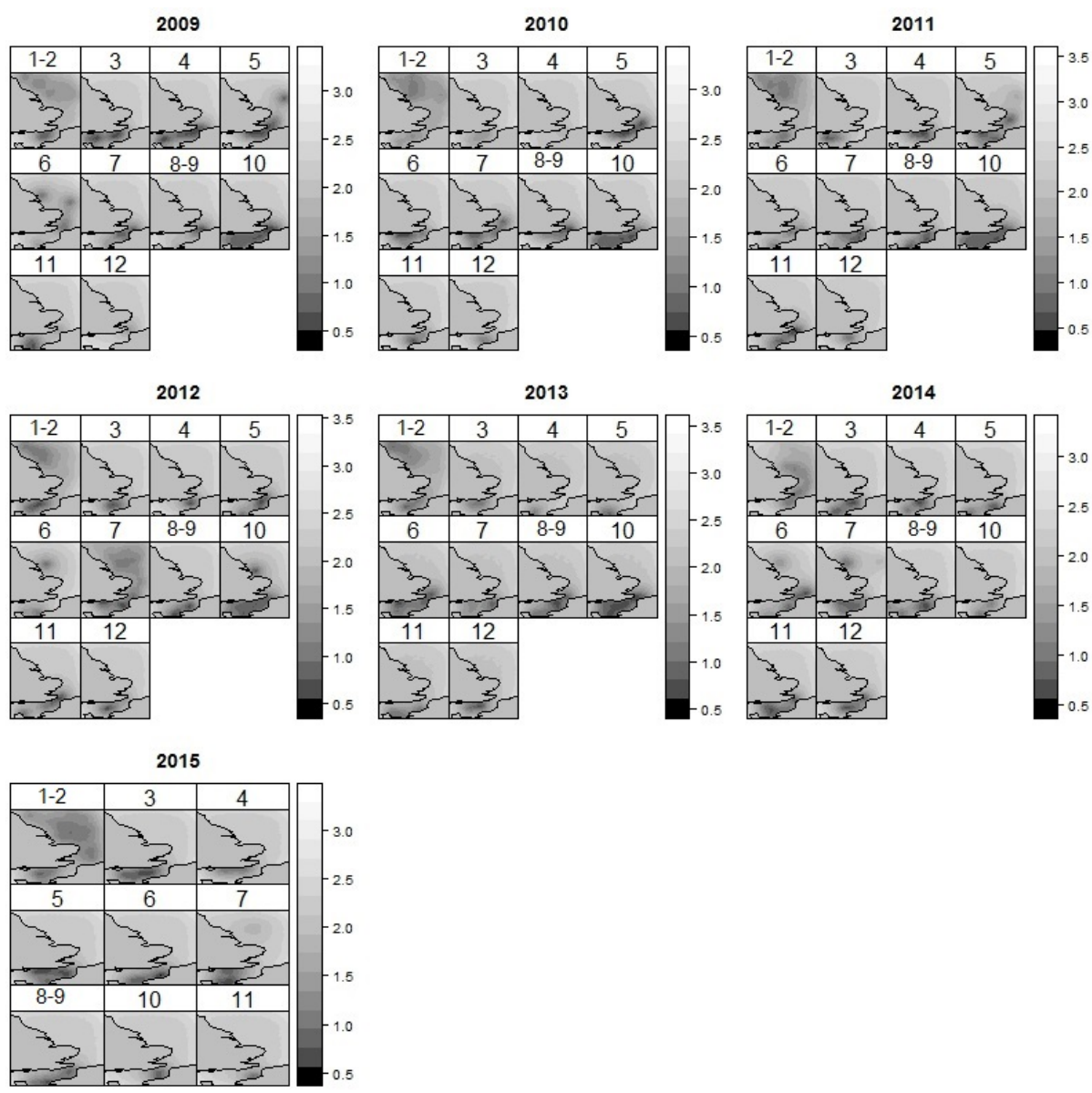
553

554

555 Figure 3 Mean (left-hand side) and standard deviation (right-hand side) of the spatial random
 556 effect at a seasonal resolution for dataset B – Positive values of the mean indicate a high
 557 density of presence data while negative values indicate a high density of absence data. The
 558 standard deviation increases with distance from the data points.

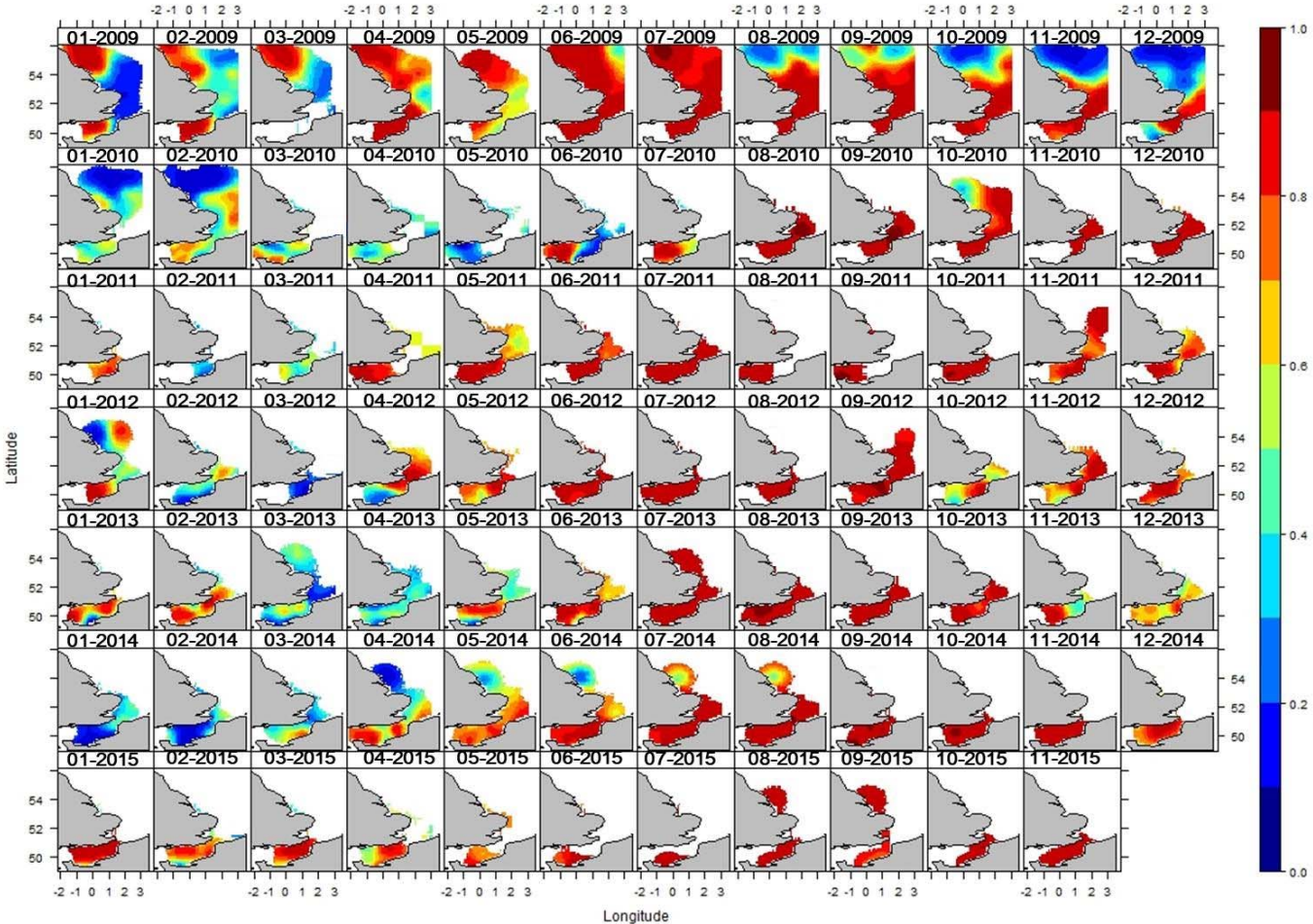


560 Figure 4 Standard deviation of the spatial random effect for dataset A. The months of January
561 and February and August and September were grouped together in order to combine the parts
562 of the IBTS survey that straddled months.

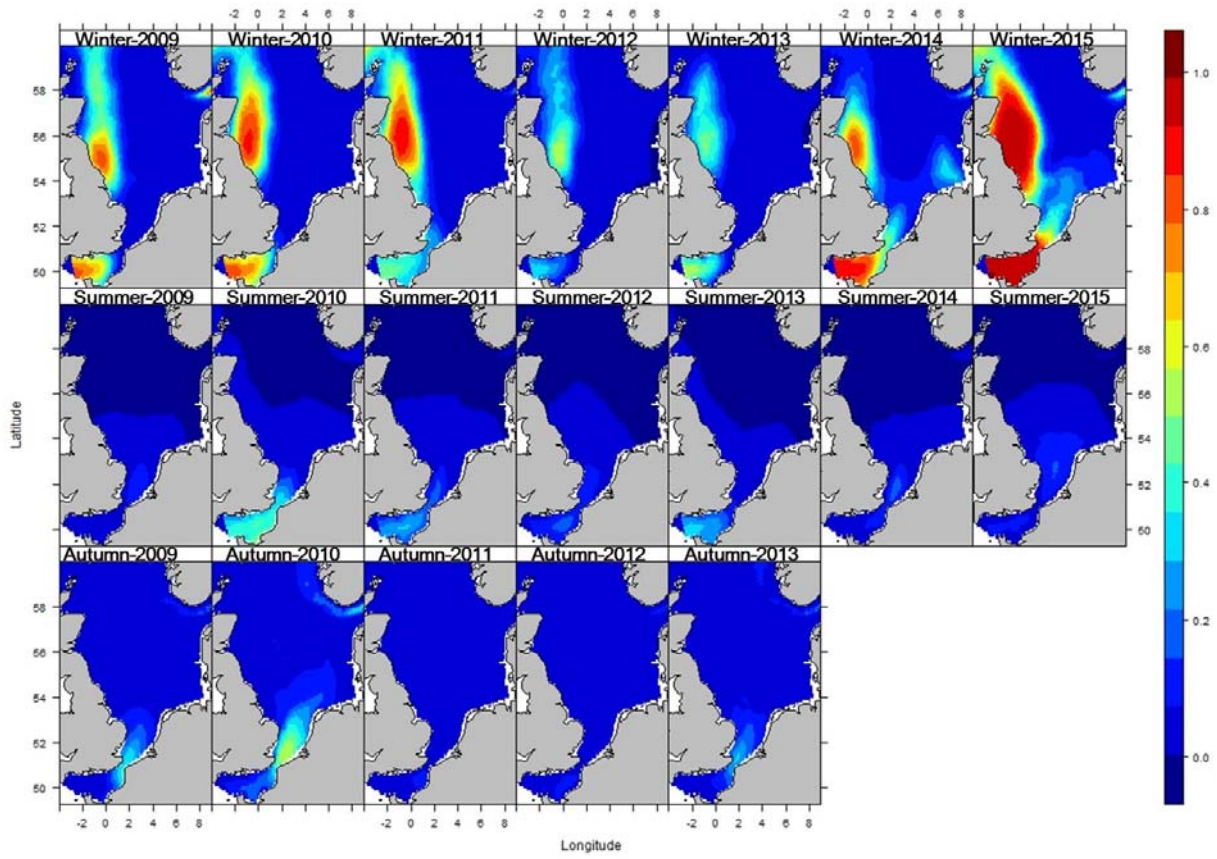


563
564
565
566

567 Figure 5 Spatial predictions of the probability of presence of striped red mullet in the Eastern English Channel and southern North Sea at a
568 monthly resolution from 2009 (top) to 2015 (bottom), as output from the best model for dataset A. White areas represent grid cells in which the
569 standard deviation was higher than the mean standard deviation (on a logit scale) (see Fig. S2).



571 Figure 6 Spatial predictions of the probability of presence of striped red mullet in the Eastern
572 English Channel and the North Sea at a seasonal resolution from 2009 (left) to 2015 (right), as
573 output from the best model for dataset B.



574
575

1 **Appendix A**

2

3 **Notes on the modelling approach**

4

5 The mixed effects models we fit in this paper fall broadly within the class of ‘empirical’ statistical
6 models as defined by Levins (1966). These types of models are in essence correlative, although
7 they may have mechanistic underpinnings related to the fundamentals of Grinnellian and Eltonian
8 niches (Hutchinson 1957; Soberón 2007; Beale et al. 2014). In lieu of the oft-lacking, detailed
9 physiological knowledge needed for parameterization of an exciting new family of process-based
10 models (e.g., Freitas et al. 2010; Jørgensen et al. 2012; Teal et al. 2012; see Peck et al. 2018 for a
11 review), correlative models, which tend to compromise generality for realism and precision
12 (Levins 1966; Dickey-Collas et al. 2014), remain widely used in ecology to explore the nature of
13 relationships between species’ distributions and biotic and abiotic factors, to build hypotheses and
14 to guide management decisions (Guisan and Thuiller 2005; Elith and Leathwick 2009; Robinson
15 et al. 2011).

16

17 Our models were fitted in a Bayesian framework in R-INLA, using the SPDE approach to capture
18 spatial and temporal dependence in the data (Rue et al. 2009; Lindgren et al. 2011). The merits of
19 the Bayesian approach for this type of hierarchical model are many (Gelfand et al. 2006; Gelman
20 and Hill 2007; Royle et al. 2007). Without reviewing these exhaustively here (see Elderd and
21 Miller 2016 for a comprehensive appraisal), we highlight the inherent way in which random effects
22 are handled as parameters of interest, resulting in fully specified probability distributions from
23 which information on the intensity and uncertainty of the effects can be drawn; the option to

24 incorporate prior knowledge based on empirical data or theory; and the ability to robustly quantify
25 and propagate uncertainty through all modelling stages. Model fitting using INLA is
26 computationally efficient, and provides accurate approximations of the posterior marginal
27 distributions of model parameters that show high concordance with MCMC simulations (Rue and
28 Martino 2007; Rue et al. 2009; Held et al. 2010). Since Lindgren and colleagues proved that a
29 continuously indexed Gaussian field described by a Matérn covariance function can be represented
30 as a discretely indexed GMRF (Rue and Held 2005; Lindgren et al. 2011), rapid development of
31 the SPDE approach within R-INLA has facilitated fitting of an expanding suite of hierarchical
32 spatial and spatiotemporal models to spatial point patterns (Krainski et al. 2016). This approach
33 has recently proven useful in analyses of georeferenced fisheries datasets, which are often data-
34 rich and where inference at the scale of point locations, rather than grids, is required (e.g.,
35 Cosandey-Godin et al. 2015; Ono et al. 2016; Ward et al. 2015).

36
37 One of the well-noted criticisms of correlative species distribution models (Elith and Leathwick
38 2009 for a review of different methods) has been their inability to adequately account for residual
39 autocorrelation in space and/or time. This situation that can violate independence assumptions in
40 regression models, leading to inference errors and/or misrepresentation of covariate importance
41 (Legendre 1993; Dormann 2007; Beale et al. 2010). The SPDE approach considers these
42 correlation structures directly, and allows great flexibility in their specification (e.g., Cosandey-
43 Godin et al. 2015). We specified temporally-independent realizations of the spatially-structured
44 error terms, but temporal dependence can easily be coded (e.g. Macdonald et al. 2018).

45

46 Our models were specific to striped red mullet in the North Sea and English Channel. However,
47 the approach used is easily adaptable to other stocks and species for which questions on the drivers
48 of distribution shifts remain open. The 20-year dataset we analyzed represents a substantial
49 compilation of georeferenced records on the environmental conditions experienced by *M.*
50 *surmuletus* across a substantial part of its range. The model outputs therefore provide a basis for
51 identifying physiological thresholds that can be used to develop more informative priors in future
52 regression models (Simpson et al. 2015), or to guide parameterization of mechanistic models (Teal
53 et al. 2018). We agree with Rochette et al. (2013) who advocate a hierarchical Bayesian framework
54 as an appealing platform upon which to meld different types of data and models together, making
55 it possible to assimilate the processes acting on different life-history phases within the one ‘full
56 life cycle’ model. We see potential for the types of models developed here to contribute to the
57 development of such a model for *M. surmuletus*.

58

59 **References**

60 Beale, C. M., Brewer, M. J., and Lennon, J. J. 2014. A new statistical framework for the
61 quantification of covariate associations with species distributions. *Methods in Ecology and*
62 *Evolution* **5**:421–432.

63 Beale, C. M., Lennon, J. J., Yearsley, J. M., Brewer, M. J., and Elston, D. A. 2010. Regression
64 analysis of spatial data. *Ecology Letters* **13**:246–264.

65 Cosandey-Godin, A., Krainski, E. T., Worm, B., and Flemming, J. M. 2015. Applying Bayesian
66 spatiotemporal models to fisheries bycatch in the Canadian Arctic. *Canadian Journal of Fisheries*
67 *and Aquatic Sciences* **12**:1–12.

- 68 Dickey-Collas, M., Payne, M. R., Trenkel, V. M., and Nash, R. D. M. 2014. Hazard warning:
69 model misuse ahead. *ICES Journal of Marine Science* **71**:2300–2306.
- 70 Dormann, C. F. 2007. Effects of incorporating spatial autocorrelation into the analysis of species
71 distribution data. *Global Ecology and Biogeography* **16**:129–138.
- 72 Elith, J., and Leathwick, J. 2009. Species distribution models: ecological explanation and
73 prediction across space and time. *Annual Review of Ecology, Evolution, and Systematics* **40**:677–
74 697.
- 75 Elder, B. D., and Miller, T. E. X. 2016. Quantifying demographic uncertainty: Bayesian methods
76 for integral projection models. *Ecological Monographs* **86**:125–144.
- 77 Freitas, V., Cardoso, J. F. M. F., Lika, K., Peck, M. A., Campos, J., Kooijman, S. A. L. M., and
78 van der Veer, H. W. 2010. Temperature tolerance and energetics: a dynamic energy budget-based
79 comparison of North Atlantic marine species. *Philosophical Transactions of the Royal Society B:*
80 *Biological sciences* **365**:3553–3565.
- 81 Gelfand, A. E., Silander Jr, J. A., Wu, S., Latimer, A., Lewis, P. O., Rebelo, A. G., and Holder, M.
82 2006. Explaining species distribution patterns through hierarchical modeling. *Bayesian Analysis*
83 **1**:41–92.
- 84 Gelman, A., and Hill, J. 2007. *Data analysis using regression and multilevel/hierarchical models*.
85 Cambridge University Press, New York, USA.
- 86 Guisan, A., and Thuiller, W. 2005. Predicting species distribution: offering more than simple
87 habitat models. *Ecology Letters* **8**:993–1009.

- 88 Held, L., Schrödle, B., and Rue, H. 2010. Posterior and cross-validators predictive checks: A
89 comparison of MCMC and INLA. Pages 91–110 in Kneib, T., and Tutz, G., editors. Statistical
90 modelling and regression structures. Physica-Verlag, Berlin, Germany.
- 91 Hutchinson, G. E. 1957. Concluding remarks. Cold Spring Harbor Symposium on Quantitative
92 Biology **22**:415–427.
- 93 Jørgensen, C., Peck, M. A., Antognarelli, F., Azzurro, E., Burrows, M. T., Cheung, W. W. L.,
94 Cucco, A., Holt, R. E., Huebert, K. B., Marras, S., McKenzie, D., Metcalfe, J., Perez-Ruzafa, A.,
95 Sinerchia, M., Fleng Steffensen, J., Teal, L. R., and Domenici, P. 2012. Conservation physiology
96 of marine fishes: advancing the predictive capacity of models. *Biology letters* **8**:900–903.
- 97 Krainski, E. T., Lindgren, F., and Simpson, D. 2016. The R-INLA tutorial on SPDE models.
98 Technical report to the Department of Mathematical Sciences, Norwegian University of Science
99 and Technology, Trondheim, Norway.
- 100 Legendre, P. 1993. Spatial autocorrelation: trouble or new paradigm? *Ecology* **74**:1659–1673.
- 101 Levins, R. 1966. The strategy of model building in population biology. *American Scientist* **54**:421–
102 431.
- 103 Lindgren, F., Rue, H., and Lindström, J. 2011. An explicit link between Gaussian fields and
104 Gaussian Markov random fields: the stochastic partial differential equation approach. *Journal of*
105 *the Royal Statistical Society: Series B (Statistical Methodology)* **73**:423–498.
- 106 Macdonald, J.I., Logemann, K., Krainski, E. T., Sigurðsson, Þ., Beale, C. M., Huse, G., Hjøllo, S.
107 S., and Marteinsdóttir, G. 2018. Can collective memories shape fish distributions? A test, linking
108 space-time occurrence models and population demographics. *Ecography* **41**:938–957.

- 109 Ono, K., Shelton, A. O., Ward, E. J., Thorson, J. T., Feist, B. E., and Hilborn, R. 2016. Space-time
110 investigation of the effects of fishing on fish populations. *Ecological Applications* **26**:392–406.
- 111 Peck, M. A., Arvanitidis, C., Butenschön, M., Canu, D. M., Chatzinikolaou, E., Cucco, A.,
112 Domenici, P., Fernandes, J. A., Gasche, L., Huebert, K. B., Hufnagl, M., Jones, M. C., Kempf, A.,
113 Keyl, F., Maar, M., Mahévas, S., Marchal, P., Nicolas, D., Pinnegar, J. K., Rivot, E., Rochette, S.,
114 Sell, A. F., Sinerchia, M., Solidoro, C., Somerfield, P. J., Teal, L. R., Travers-Trolet, M., and van
115 de Wolfshaar, K. E. 2018. Projecting changes in the distribution and productivity of living marine
116 resources: A critical review of the suite of modelling approaches used in the large European project
117 VECTORS. *Estuarine, Coastal and Shelf Science* **201**:40–55.
- 118 Robinson, L. M., Elith, J., Hobday, A. J., Pearson, R. G., Kendall, B. E., Possingham, H. P., and
119 Richardson, A. J. 2011. Pushing the limits in marine species distribution modelling: lessons from
120 the land present challenges and opportunities. *Global Ecology and Biogeography* **20**:789–802.
- 121 Rochette, S., Le Pape, O., Vigneau, J., and Rivot, E. 2013. A hierarchical Bayesian model for
122 embedding larval drift and habitat models in integrated life cycles for exploited fish. *Ecological*
123 *Applications* **23**:1659–1676.
- 124 Royle, J., Kéry, M., Gautier, R., and Schmid, H. 2007. Hierarchical spatial models of abundance
125 and occurrence from imperfect survey data. *Ecological Monographs* **77**:465–481.
- 126 Rue, H., and Held, L. 2005. Gaussian Markov random fields: theory and applications. Monographs
127 on statistics and applied probability volume 104. Chapman & Hall, London, UK.
- 128 Rue, H., and Martino, S. 2007. Approximate Bayesian inference for hierarchical Gaussian Markov
129 random fields models. *Journal of Statistical Planning and Inference* **137**:3177–3192.

- 130 Rue, H., Martino, S., and Chopin, N. 2009. Approximate Bayesian inference for latent Gaussian
131 models by using integrated nested Laplace approximations. *Journal of the Royal Statistical*
132 *Society: Series B (Statistical Methodology)* **71**:319–392.
- 133 Simpson, D. P., Rue, H., Martins, T. G., Riebler, A., and Sørbye, S. H. 2015. Penalising model
134 component complexity: A principled, practical approach to constructing priors. arXiv 1403.4630
- 135 Soberón, J. 2007. Grinnellian and Eltonian niches and geographic distributions of species. *Ecology*
136 *Letters* **10**:1115–1123
- 137 Teal, L. R., van Hal, R., van Kooten, T., Ruardij, P., and Rijnsdorp, A. D. 2012. Bio-energetics
138 underpins the spatial response of North Sea plaice (*Pleuronectes platessa* L.) and sole (*Solea solea*
139 L.) to climate change. *Global Change Biology* **18**:3291–3305.
- 140 Teal, L. R. et al. 2018. Physiology-based modelling approaches to characterize fish habitat
141 suitability: their usefulness and limitations. *Estuarine, Coastal and Shelf Science* **201**:56–63.
- 142 Ward, E. J., Jannot, J. E., Lee, Y., Ono, K., Shelton, A. O., Thorson, J. T. 2015. Using
143 spatiotemporal species distribution models to identify temporally evolving hotspots of species co-
144 occurrence. *Ecological Applications* **25**:2198–2209.